Proposal for a digital converter of analog magnetic signals

Christian Ertler[a] and Jaroslav Fabian[b]
Institute for Theoretical Physics, University of Regensburg, D-93040 Regensburg, Germany

(Received 10 July 2006; accepted 18 September 2006; published online 10 November 2006)

A device which converts analog magnetic signals directly into digital information is proposed. The device concept is based on the monostable-bistable transition logic element, which consists of two resonant tunneling diodes (load and driver) connected in series and employs the monostable to bistable working point transition of the circuit. Using a magnetic resonant tunneling diode as the driver allows to control the resulting working point of the bistable region by an external magnetic field leading either to high or low output voltage of the circuit, effectively realizing what could be called digital magnetoresistance. © *2006 American Institute of Physics*. [DOI: 10.1063/1.2374800]

Since the realization of magnetic III-V semiconductors[1] substantial progress has been made in pushing the transition temperature to even higher values, strongly nurturing the hope for technically applicable room temperature magnetic semiconductors in the near future. Much has been done to exploit the possibilities offered by these materials in diverse spintronic device concepts.[2] For instance, in magnetic resonant tunneling diodes[3–9] (m-RTDs) or magnetic multiple quantum well diodes,[10,11] the transmission can strongly depend on the spin orientation of the electrons at the Fermi level, which allows to use the diodes as spin filters and detectors. The quantum well of RTDs can be formed either by a ferromagnetic semiconductor[12–14] or by dilute magnetic semiconductors (DMSs),[15] which exhibit giant g factors. Magnetic devices provide the interesting opportunity of realizing nonvolatile reprogrammable logic elements. A nonvolatile ferromagnet/superconductor switch based on Andreev reflections was proposed in Ref. 16.

Nonmagnetic RTDs have been used for multiple valued logic and multiple logic functions with multiple input and/or output,[17] due to their specific N-shaped current-voltage (IV) characteristics and their extremely high-speed potential. In 1993 Maezawa and Mizutani proposed the monostable-bistable transition logic element (MOBILE).[18] The concept was extended to multistable elements[19,20] and applications to ultrahigh-speed analog to digital converters were demonstrated.[21] The MOBILE device consists of two nonmagnetic RTDs, a load and a driver, which are connected in series. In this letter we demonstrate that MOBILE circuits with m-RTDs can be used as digital converters of analog magnetic signals by realizing digital magnetoresistance (DMR): for a continuous change of the magnetic field through a *controlled* threshold the output electrical characteristics such as voltage exhibit discrete jumps. A nice related effect of the MOBILE has been realized by Hanbicki *et al.*:[22] a nonmagnetic driver RTD is shunted with a metallic giant magnetoresistance resistor, allowing for current modulations through the RTD. This fascinating phenomenon makes DMR-MOBILEs serious candidates for magnetic reading devices.

Figure 1 shows the schematic circuit diagram for a DMR-MOBILE, in which the driver is a m-RTD. The basic concept of the operation of a MOBILE is to drive the circuit by an oscillating input voltage V_{in} to produce the transition between the monostable and bistable working points regime of the circuit.[18] In the bistable regime there is a stable dc working point at a low voltage and another at a high voltage. Which of them is actually realized after the transition by the circuit is determined by the difference of the peak currents between the two RTDs. If the load peak current is lower than the driver peak current the circuit output voltage is low, and vice versa. The load line diagrams of both cases are schematically shown in Fig. 2. The upper (lower) diagram shows the case when the peak current of the load is smaller (higher) than that of the driver device. By increasing the input voltage the mirrored IV of the load is shifted rightwards. The intersection points with the driver IV are the candidates for stable dc working points of the circuit. The number of crossing points changes from 1 at low input voltages (monostable regime) up to 3 at high input voltages (bistable regime). However, the crossing point in the negative differential resistance (NDR) region proves to be unstable by the following criterion. For small fluctuations δV_l and δV_d from the equilibrium load and driver voltages V_l and V_d (with the constraint $V_l+V_d=V_{\text{in}}$), a Rayleigh dissipative potential can be defined as

$$\delta P = \frac{1}{2}[G_l(\delta V_l)^2 + G_d(\delta V_d)^2] = \frac{1}{2}(G_l + G_d)(\delta V_d)^2, \qquad (1)$$

where G_l and G_d denote the differential conductances at the working points of the load and driver, respectively. For a stable system, the dissipative potential must be a positive definite form leading to the stability criterion $G_l+G_d>0$,

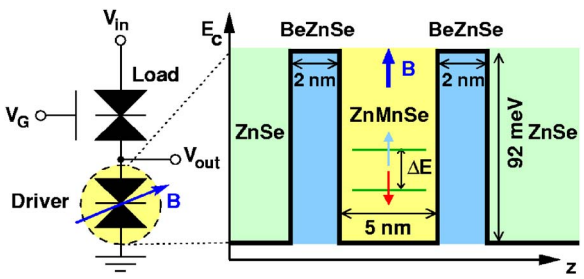

FIG. 1. (Color online) Left: Circuit configuration of the proposed DMR-MOBILE. The load is a conventional RTD, whose peak current can be modified by an external gate voltage V_G. The driver device consists of a magnetic RTD [here made of a Zn(Be, Mn)Se material system]. The peak current of the driver is controlled by the magnetic field. Right: Schematic conduction band profile of the magnetic RTD used in the numerical simulations discussed in the text.

[a]Electronic mail: christian.ertler@physik.uni-regensburg.de
[b]Electronic mail: jaroslav.fabian@physik.uni-regensburg.de

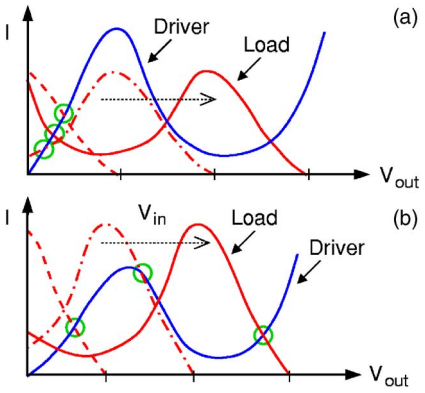

FIG. 2. (Color online) Schematic load line diagrams for the case of a higher (a) and a lower (b) driver peak current compared to the load peak value. The mirrored load *IV* characteristic is shifted from the left (dashed line) to the right (solid line) when the input voltage V_{in} is increased. The dot-dashed line refers to an intermediate input voltage. The actual (stable) working point of the circuit is marked by a circle.

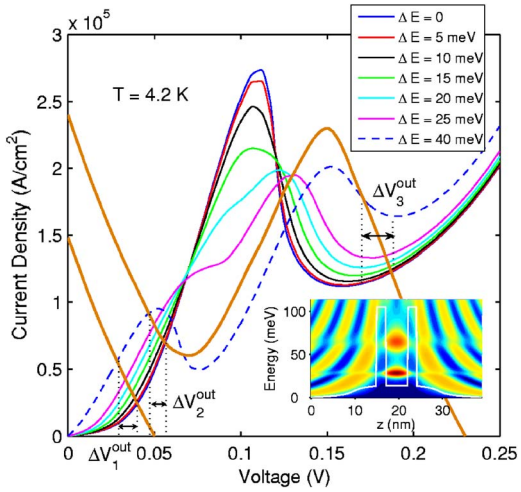

FIG. 3. (Color online) Current-voltage characteristics of the magnetic RTDs at the temperature of T=4.2 K for different Zeeman energy splittings ΔE. The thick solid lines indicate the mirrored *IV* curve of the load RTD for low and high input voltages. The inset shows a contour plot of the local density of states vs energy and growth direction z at zero bias and ΔE=40 meV. The solid line in the inset indicates the conduction band profile. The two spin resonances are visible by the large density (dark) in the well.

which is clearly violated in the NDR region. A more detailed analysis (including the dynamic behavior of the circuit) of the stability of working points in RTDs is given in Refs. 23 and 24. As illustrated in Fig. 2(a) the actual working point (marked by a circle) remains always in the low voltage area if the load peak current is smaller than the driver peak value. For the opposite case, displayed in Fig. 2(b), the working point can overcome the driver peak voltage, resulting in a high output voltage for high input voltages. The difference in the peak currents can be very small to perform the switching between the low and high voltage states, as the transition is in some sense analogous to a second-order phase transition.[18]

For our proposed device, DMR-MOBILE, we suggest to use a conventional RTD for the load but to replace the driver by a m-RTD as illustrated in Fig. 1. This allows, as we will see below, to change the peak current of the driver by an external magnetic field. In addition, the peak current of the load is tunable by an external gate voltage.[18] The schematic conduction band profile of the m-RTD is also shown in Fig. 1. The quantum well is considered to be made of the DMS material ZnMnSe, whereas the barriers are formed by Be-doped ZnSe. The barrier height is assumed to be 92 meV, which is about 23% of the band gap difference between ZnBeSe and ZnSe. The active region of the structure is sandwiched between two n-doped ZnSe layers with $n \approx 10^{18}$ cm^{-3} including a 5 nm thick undoped buffer layer. Similar all II-VI semiconductor m-RTDs have already been experimentally investigated.[3]

Due to the giant g factor in DMSs an external magnetic field B causes a giant Zeeman energy splitting of the conduction band. The energy difference of the spin up and down states ΔE can be expressed by a modified Brillouin function B_s:[9]

$$\Delta E = x_{\text{eff}} N_0 \alpha s B_s(g_{\text{Mn}} s \mu_B B / k_B T_{\text{eff}}), \tag{2}$$

where x_{eff} is the effective concentration of Mn ions, $N_0\alpha$ =0.26 eV is the *sp-d* exchange constant for conduction electrons, s=5/2 is the Mn spin, g_{Mn}=2.00 is the Mn g factor, μ_B labels the Bohr magneton, k_B denotes the Boltzmann constant, and T_{eff} is an effective temperature. Hence, the DMS gives rise to a spin dependent potential energy term in the electron Hamiltonian, $U_\sigma(z)=\sigma\Delta E(z)$, with z denoting the growth direction of the heterostructure and $\sigma=\pm 1/2$ or $(\uparrow,\downarrow)$ labeling the spin quantum number. Assuming coherent transport through the m-RTD we calculate the spin dependent current by numerically solving the single band effective mass Schrödinger equation. Space charge effects are self-consistently taken into account in our numerical simulations by calculating the conduction band profile from the Poisson equation. The spin dependent current density J_σ is then calculated by the Tsu-Esaki formula[25]

$$J_\sigma = \frac{e m^* k_B T}{4\pi^2 \hbar^3} \int_0^\infty dE_z T_\sigma(E_z) g(E_z),$$

$$g(E_z) = \ln\left[\frac{1+\exp(E_F - E_z/k_B T)}{1+\exp((E_F - eV_a - E_z)/k_B T)}\right], \tag{3}$$

where e is the elementary charge, $m^*=0.145m_0$ is the effective mass of the electrons with m_0 denoting the free electron mass, $\hbar$ labels the reduced Planck constant, T_σ denotes the spin dependent transmission function, E_z is the longitudinal energy of the electrons, E_F denotes the Fermi energy of the left lead, and V_a is the voltage applied to the right lead.

At low temperatures (we set T=4.2 K as in Ref. 3) the Zeeman splitting is of the order of 10 meV for practical magnetic fields of 1–2 T and Mn concentrations of about 8%. The obtained *IV* characteristics for the m-RTD for different Zeeman splittings are displayed in Fig. 3. The inset of Fig. 3 shows a contour plot of the local density of states at zero bias for ΔE=40 meV, with the solid line indicating the self-consistent conduction band profile. The upward band bending at equilibrium is caused by the undoped buffer layers. The local density of states clearly demonstrates the Zeeman splitting of the quasibound energy state in the quantum well. Since we consider a positive applied magnetic field the lower and upper energy states correspond to spin down and spin up, respectively. For high magnetic fields the Zeeman splitting becomes also observable in the *IV* characteristics leading to two separated current peaks. However, most important with respect to the functionality of the proposed DMR device is the fact that the peak current is appreciably decreased by an applied external magnetic field. The mirrored *IV* charac-

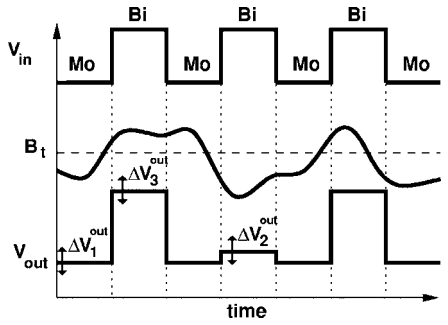

FIG. 4. Scheme of the operation principle of the DMR-MOBILE. The vertical dotted lines indicate the points of time when a mono to bistable transition is performed. The output voltages fluctuate within the intervals ΔV_i^{out}, $i=1,2,3$.

teristics of the nonmagnetic load device for low (monostable regime) and high (bistable regime) input voltages, respectively, are indicated by the thick solid lines. As illustrated in Fig. 3 for fixed low and high input voltages, the output voltage is restricted to three different intervals $\Delta V_i^{\text{out}}, i=1,2,3$. The high voltages interval ΔV_3^{out} are considerably separated from the low voltages intervals ΔV_1^{out} and ΔV_2^{out} which allows a digital interpretation of the output voltage. The magnetic field dependence of m-RTDs has been already seen experimentally in Ref. 3.

To utilize the influence of the magnetic field on the driver peak current, we suggest the following operation principle of our DMR-MOBILE, which is schematically visualized in Fig. 4. Let us assume that the two RTDs of the MOBILE are of such kind that the driver peak current is higher than the load peak current at zero magnetic field. By applying an external magnetic field the driver peak current is reduced and at some threshold value B_t it becomes smaller than the load peak current. This threshold is determined by the value of the field in which the two peak currents are equal. The magnitude of B_t can be conveniently controlled by V_G.[18] The circuit is assumed to be driven by an oscillating input voltage which continually performs a transition between the mono- and bistable regimes. For simplicity we consider a rectangular input signal in Fig. 4. If the magnetic field is higher (lower) than the threshold field B_t at the moment of the transition from the monostable to the bistable regime, the output voltage is high (low), which leads to a direct digital conversion of the magnetic signal.

The question of how fast this conversion operation can be performed is closely connected to the subtle question of error rates in MOBILEs. The dynamical response of a m-RTD on a sudden change in the external magnetic field is similar to the response on an abrupt change of the applied voltage in nonmagnetic RTDs. Both operations lead effectively to a redistribution of the quasibound states in the quantum well, which happens on a time scale of the order of hundred of femtoseconds. However, the switching transition time of RTDs is dominated by the *RC* time constant, which limits the switching performance to a few picoseconds.[26] These considerations suggest that the error rates in magnetic and conventional MOBILEs are comparable. In particular, parasitic capacitances are a possible source for an erroneous mono to bistable transition, since they can influence the peak current values.[27] Experiments show that the circuit randomly outputs high and low in the transition region.[28] These fluctuations might be in part due to external electric noise. Transient analysis of the conventional MOBILE structure based on equivalent circuit models[29] reveals that an error-free transition with clock rise times on the order of the *RC* time of the RTD is possible if the output capacitance C_{out} is reduced appropriately. A rough approximation, yields $C_{\text{out}}<(k-1)C_{\text{RTD}}$,[29] where k is the ratio of the load to driver peak current and C_{RTD} is an average capacitance of the RTD. Recently, an ultrahigh frequency operation of MOBILEs up to 100 GHz has been demonstrated by employing a symmetric clock configuration.[30] Hence, the proposed DMR-MOBILE scheme might be potentially used, e.g., as a very fast read head in conventional hard disks.

To summarize, we propose a DMR-MOBILE which converts analog magnetic signals directly into digital electrical information. The device is essentially a MOBILE, where the driver device is replaced by a m-RTD made of a DMS material. How high ΔE must there be for practical operations? One expects (and our simulations confirm) that ΔE should be of the order of $k_B T$. With the current materials this limits the operation of the DMR-MOBILE to temperatures lower than perhaps 150 K.

This work has been supported by the Deutsche Forschungsgesellschaft SFB 689. The authors thank K. Maezawa and T. Waho for valuable discussions.

[1] H. Ohno, Science **281**, 951 (1998).
[2] I. Žutić, J. Fabian, and S. Das Sarma, Rev. Mod. Phys. **76**, 323 (2004).
[3] A. Slobodskyy, C. Gould, T. Slobodskyy, C. R. Becker, G. Schmidt, and L. W. Molenkamp, Phys. Rev. Lett. **90**, 246601 (2003).
[4] T. Hayashi, M. Tanaka, and A. Asamitsu, J. Appl. Phys. **87**, 4673 (2000).
[5] P. Bruno and J. Wunderlich, J. Appl. Phys. **84**, 978 (1998).
[6] I. Vurgaftman and J. R. Meyer, Phys. Rev. B **67**, 125209 (2003).
[7] A. Voskoboynikov, S. S. Lin, C. P. Lee, and O. Tretyak, J. Appl. Phys. **87**, 387 (2000).
[8] A. G. Petukhov, A. N. Chantis, and D. O. Demchenko, Phys. Rev. Lett. **89**, 107205 (2002).
[9] N. N. Beletskii, G. P. Berman, and S. A. Borysenko, Phys. Rev. B **71**, 125325 (2005).
[10] D. Sánchez, A. H. MacDonald, and G. Platero, Phys. Rev. B **65**, 035301 (2001).
[11] C. Ertler and J. Fabian, e-print cond-mat/0606531.
[12] A. Oiwa, R. Moriya, Y. Kashimura, and H. Munekata, J. Magn. Magn. Mater. **276**, 2016 (2004).
[13] J. Furdyna, T. Wojtowicz, X. Liu, K. M. Yu, W. Walukiewicz, I. Vurgaftman, and J. R. Meyer, J. Phys.: Condens. Matter **16**, S5499 (2004).
[14] T. Dietl, Semicond. Sci. Technol. **17**, 377 (2002).
[15] J. K. Furdyna, J. Appl. Phys. **64**, R29 (1988).
[16] B. Nadgorny and I. I. Mazin, Appl. Phys. Lett. **80**, 3973 (2002).
[17] K. Maezawa and A. Förster, *Nanoelectronics and Information Technology* (Wiley-VCH, 2003), pp. 407–424.
[18] K. Maezawa and T. Mizutani, Jpn. J. Appl. Phys., Part 2 **32**, L42 (1993).
[19] T. Waho, *Proceedings of the 25th IEEE International Symposium on Multiple-Valued Logic* (IEEE, New York, 1995), pp. 130–138.
[20] T. Waho, K. J. Chen, and M. Yamamoto, IEEE J. Solid-State Circuits **33**, 268 (1998).
[21] K. Hattori, Y. Takamatsu, and T. Waho, IEICE Trans. Electron. **E85-C**, 586 (2002).
[22] A. Hanbicki, R. Magno, S. F. Cheng, Y. D. Park, A. S. Bracker, and B. T. Jonker, Appl. Phys. Lett. **79**, 1190 (2001).
[23] C. Kidner, I. Mehdi, J. R. East, and G. I. Haddad, Solid-State Electron. **34**, 149 (1991).
[24] W. F. Chow, *Principles of Tunnel Diode Circuits* (Wiley, 1964), Chap. 4.
[25] R. Tsu and L. Esaki, Appl. Phys. Lett. **22**, 562 (1973).
[26] S. K. Diamond, E. Özbay, M. J. W. Rodwell, D. M. Bloom, Y. C. Pao, and J. Harris, Appl. Phys. Lett. **54**, 153 (1989).
[27] T. Waho (private communication).
[28] K. Maezawa (private communication).
[29] K. Maezawa, Jpn. J. Appl. Phys., Part 1 **34**, 1213 (1995).
[30] K. Maezawa, H. Sugiyama, S. Kishimoto, and T. Mizutani, International Conference on InP and Related Materials Conference Proceedings, 2006, pp. 46–49.